

pubs.acs.org/Biomac Article

Poly(pro-curcumin) Materials Exhibit Dual Release Rates and Prolonged Antioxidant Activity as Thin Films and Self-Assembled Particles

Ruiwen Chen, Jessica L. Funnell, Geraldine B. Quinones, Marvin Bentley, Jeffrey R. Capadona, Ryan J. Gilbert,* and Edmund F. Palermo*



Cite This: Biomacromolecules 2023, 24, 294-307



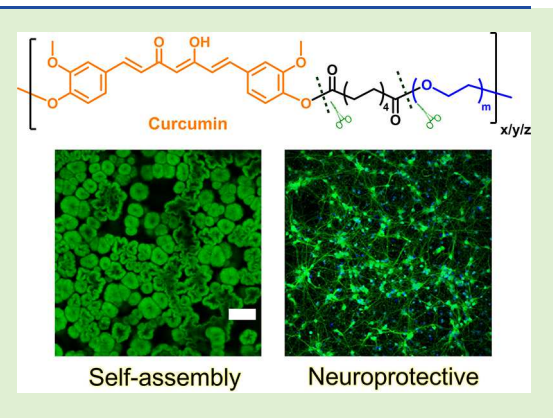
ACCESS I

III Metrics & More

Article Recommendations

Supporting Information

ABSTRACT: Curcumin is a natural polyphenol that exhibits remarkable antioxidant and anti-inflammatory activities; however, its clinical application is limited in part by its physiological instability. Here, we report the synthesis of curcumin-derived polyesters that release curcumin upon hydrolytic degradation to improve curcumin stability and solubility in physiological conditions. Curcumin was incorporated in the polymer backbone by a one-pot condensation polymerization in the presence of sebacoyl chloride and polyethylene glycol (PEG, $M_n=1$ kDa). The thermal and mechanical properties, surface wettability, self-assembly behavior, and drug-release kinetics all depend sensitively on the mole percentage of curcumin incorporated in these statistical copolymers. Curcumin release was triggered by the hydrolysis of phenolic esters on the polymer backbone, which was confirmed using a PEGylated curcumin model compound, which represented a putative repeating unit within the polymer. The release rate of curcumin was controlled by the



hydrophilicity of the polymers. Burst release (2 days) and extended release (>8 weeks) can be achieved from the same polymer depending on curcumin content in the copolymer. The materials can quench free radicals for at least 8 weeks and protect primary neurons from oxidative stress in vitro. Further, these copolymer materials could be processed into both thin films and self-assembled particles, depending on the solvent-based casting conditions. Finally, we envision that these materials may have potential for neural tissue engineering application, where antioxidant release can mitigate oxidative stress and the inflammatory response following neural injury.

■ INTRODUCTION

Curcumin is a natural polyphenol extracted from the rhizomes of the turmeric plant. ^{1,2} For centuries, it has been widely consumed as a dye and spice in the food industry. ^{3,4} In addition to culinary uses, curcumin shows remarkable antioxidant, anti-inflammatory, neuroprotective, and antimicrobial bioactivities in vitro. ^{5,6} The neuroprotective activities of curcumin are of particular interest, as various in vitro and in vivo nervous system injury models have shown that curcumin protects against lipid peroxidation ⁷ and peroxynitrite damage. ⁸ However, clinical application of curcumin is restricted because of its low bioavailability and physiological instability. ^{9,10} The hydrophobic nature of curcumin restricts its uptake by cells and reduces the drug's bioactivity and therapeutic effect. ^{9,10}

Ongoing efforts have been focused on increasing the aqueous solubility of curcumin by encapsulating it in the hydrophobic cores of liposomes, $^{11-13}$ micelles, 14,15 β -cyclodextrins, $^{16-18}$ and nanoparticles. $^{19-22}$ Nanocarriers such as cellulose nanocrystals, 23 mesoporous silica nanoparticles, 24 and polyNIPAM nanogel 25 have also been developed featuring solubilization and triggered release of curcumin in response to

heat^{23,25} or pH.²⁴ Physically incorporating curcumin in such delivery vehicles allows for solubilization of the drug. However, because of the lack of covalent bonds between curcumin and the carrier materials, the complex destabilizes during administration, which leads to a burst release of curcumin when the structure is compromised.^{26–28}

Another strategy to enhance the solubility and long-term stability of curcumin is to conjugate the reactive phenol groups to the side chains of polyethylene glycol, ^{29,30} hyaluronic acid, ^{31–33} sodium alginate, ³⁴ or xylan. ³⁵ The diketone group in curcumin can also be functionalized by interacting with polymers bearing boronic acids ^{36,37} or complexation with metal ions. ^{38,39} Because the carrier polymers in drug-polymer

Received: September 19, 2022 Revised: November 28, 2022 Published: December 13, 2022





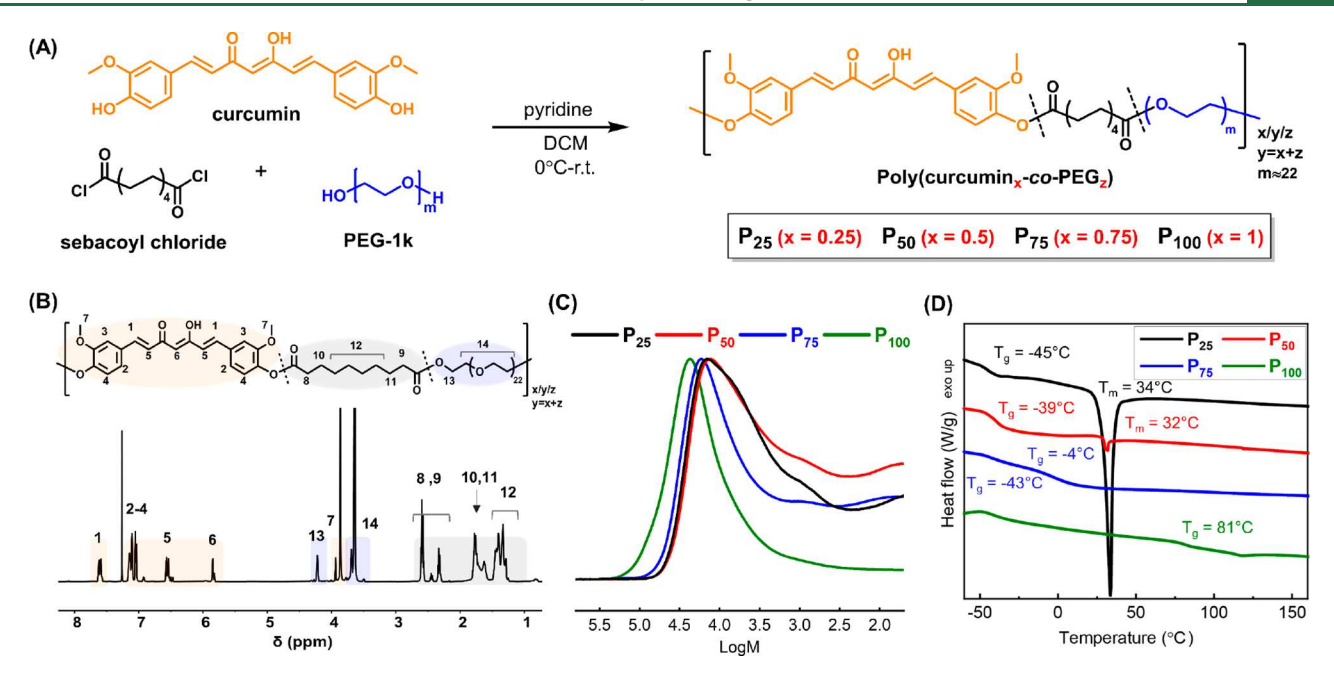


Figure 1. (A) Synthesis of poly(curcumin-co-PEG) series. (B) Representative ¹H NMR spectrum of poly(curcumin-co-PEG) P₇₅ in CDCl₃. (C) GPC trace and (D) DSC curve of poly(curcumin-co-PEG) series.

conjugates are usually pharmaceutically inactive and only serve as a scaffold, drug loading is limited. 46,41 Higher drug loading can be achieved by directly incorporating curcumin into the polymer's chemical structure, where such poly(pro-drugs) act both as the carrier matrix material and a depot of the drug itself.40 Curcumin-containing polyacetals,42,43 polyoxalates, polycarbonates, 45,46 polyurethane, 47 and polyesters 43,48 have been reported, and the release of curcumin from these materials were either rapid (<30 h)⁴⁴ or sustained (2–80 days), 42,43,45,46 depending on the stability of the linker chemistry used to enchain the drug molecules. However, for many biomedical applications, a dual-stage curcumin release profile that exhibits both an initial burst and a prolonged release may be desirable. For example, in the case of intracortical microelectrodes, neural probe implantation elicits an inflammatory response that leads to neuronal loss and the formation of a glial scar around the implant. 49-51 Ideally, a burst release of curcumin could address the initial injury caused by implantation, while sustained release of curcumin could help mitigate the long-term inflammation. To that end, we report an innovative series of poly(curcumin-co-PEG) materials that revealed certain formulations with both a burst release (2 days) and extended release (>8 weeks) of curcumin. The copolymers were synthesized by one-pot polycondensation of curcumin in the presence of sebacoyl chloride and PEG (average $M_n \approx 1000$ Da) (Figure 1A). Because of the difference in relative reactivities of phenol and hydroxyl groups, we expect a high degree of compositional drift in this system: that is, the sequence of curcumin and PEG units along the copolymer chain is likely nonuniform, with substantial blockor gradientlike compositional profiles. This blocky copolymer sequence would likely have a propensity to spontaneously selfassemble in solution. We report a comprehensive study on the materials properties, self-assembly behavior, and drug release profile of poly(curcumin-co-PEG) copolymers. Degradation kinetics of the copolymers were investigated by modulating the hydrolysis of a model compound under physiological conditions. The ability of poly(curcumin-co-PEG) copolymers

to neutralize free radicals and to protect cortical neurons from oxidative stress, via hydrogen peroxide insult, were also assessed.

■ EXPERIMENTAL SECTION

Synthesis. P₁₀₀ was synthesized following a reported procedure⁴⁸ with minor modifications. Dry pyridine (386 μ L, 4.78 mmol, 2.20 equiv) was added to a solution of curcumin (800 mg, 2.17 mmol, 1.00 equiv) in dry DCM (16.7 mL, [curcumin] = 0.130 M). The solution was cooled to 0 °C, and sebacoyl chloride (489 μ L, 2.17 mmol, 1.00 equiv) was added dropwise. The mixture was warmed to room temperature and stirred for an additional 1 h. It should be noted that a long reaction time may have caused polymer to crash out of solution. The crude product was diluted with DCM (30 mL) and washed with 0.1 M HCl (50 mL \times 3) and brine (50 mL). The organic layer was dried over anhydrous Na2SO4, concentrated on a rotary evaporator, and precipitated into methanol. The dissolution-precipitation process was repeated twice using chloroform-methanol. When full dissolution was not observed, the chloroform solution was filtered through 1 μ m PTFE syringe filters before precipitation (yellow solid, 0.90 g, 77%, peak MW = 23.0 kDa measured by GPC).

 P_{75} : Anhydrous pyridine (386 μL, 4.78 mmol, 2.20 equiv) was added to a solution of curcumin (600 mg, 1.63 mmol, 0.750 equiv) and PEG1000 (543 mg, 0.543 mmol, 0.250 equiv) in dry DCM (16.7 mL, [curcumin+PEG] = 0.130 M). The solution was cooled over ice, and sebacoyl chloride (489 μL, 2.17 mmol, 1.00 equiv) was added dropwise. The mixture was warmed to room temperature and stirred for an additional 80 min. The crude product was diluted with DCM and washed with 0.1 M HCl (50 mL × 3) and brine (50 mL). The organic layer was dried over anhydrous Na₂SO₄, concentrated on a rotary evaporator, and precipitated into cold methanol. The dissolution–precipitation process was repeated twice (yellow solid, 1.02 g, 68%, peak MW = 18.4 kDa measured by GPC).

 P_{50} : Anhydrous pyridine (290 μL, 3.58 mmol, 2.20 equiv) was added to a solution of curcumin (300 mg, 0.814 mmol, 0.500 equiv) and PEG1000 (814 mg, 0.814 mmol, 0.500 equiv) in dry DCM (1.63 mL, [curcumin] = 0.500M). Sebacoyl chloride (366 μL, 1.63 mmol, 1.00 equiv) was added dropwise at 0 °C. The mixture was warmed to room temperature and stirred for 24 h. The crude product was diluted with DCM and washed with 0.1 M HCl (50 mL × 3) and brine (50 mL). The organic layer was dried over anhydrous Na₂SO₄,

concentrated on a rotary evaporator, and precipitated into cold diethyl ether (sticky yellow solid, 0.77 g, 56%, peak MW = 14.8 kDa measured by GPC)

P₂₅: Anhydrous pyridine (386 μL, 4.78 mmol, 2.20 equiv) was added to a solution of curcumin (200 mg, 0.543 mmol, 0.250 equiv) and PEG1000 (1.63 g, 1.63 mmol, 0.75 equiv) in dry DCM (2.17 mL, [curcumin] = 0.250 M). Sebacoyl chloride (489 μL, 2.17 mmol, 2.00 equiv) was added dropwise at 0 °C. The mixture was warmed to room temperature and stirred for 48 h. The crude product was diluted with DCM and washed with 0.1 M HCl (50 mL \times 3) and brine (50 mL). The organic layer was dried over anhydrous Na₂SO₄, concentrated on a rotary evaporator, and precipitated into cold diethyl ether. The dissolution—precipitation process was repeated twice (yellow solid, 1.27 g, 58%, peak MW = 15.5 kDa measured by GPC).

Detailed descriptions of the material and methods, characterization data (including the synthesis of model compound), fabrication of thin films and self-assembly, biological assays, and microscopy procedures are included in the Supporting Information.

RESULTS AND DISCUSSION

Synthesis and Characterization of Poly(curcumin-co-PEG). Four different poly(curcumin-co-PEG) polyesters were synthesized by condensation polymerization of curcumin and PEG in the presence of sebacoyl chloride and pyridine in varying molar ratios (100, 75, 50, and 25 mol % curcumin) (Figure 1A). These poly(curcumin-co-PEG) polyester materials are referred to as P_x , where x is the molar percentage of curcumin in the above to a space of curcumin 0.25-co-PEG0.75. The structure of the copolymers was characterized by 1 H NMR spectroscopy (Figure 1B and S1), which confirmed the target structures were obtained and that the molar ratio of curcumin in each copolymer was close to the theoretical feed content to within $\leq 10\%$ error (Table 1).

Table 1. Experimental Curcumin Loading, Molecular Weight (M_p) , Polydispersity (D), Glass Transition Temperatures (T_g) , and Melting Point (T_m) of Poly(curcumin-co-PEG)

	curcumin mol % (experimental) ^a	$M_{ m p} m (kDa)$	Ð	T _g (°C)	$T_{\rm m}$ (°C)
P ₂₅	22 ± 1	15.5	2.9	-45	34
P_{50}	44 ± 1	14.8	2.9	-39	32
P_{75}	65 ± 2	18.4	2.5	-43, -4	
P_{100}	91 ± 1	23.0	2.4	81	

"Mole fraction of curcumin was determined on the basis of peak integration in ¹H NMR spectra (Figure S1).

The molecular weight distribution in each case was analyzed by GPC in THF relative to PS standards (Figure 1C), which showed that each of the copolymers possess a peak molecular weight $M_p = \sim 14-23$ kDa, and that their chain length dispersity ranges from 2.4 to 2.9 (Table 1). The GPC chromatograms of P_{25} , P_{50} , and P_{75} show tailing toward the low-molecular-weight side. This is originated from the polydisperse nature of PEG-1k used as a comonomer. Differential scanning calorimetry (DSC) data reveal that the thermal transitions are highly dependent on copolymer composition (Figure 1D). As expected, the copolymers exhibit higher glass transition temperatures (T_g) with increased molar ratio of the rigid curcumin units relative to the flexible PEG-1k content. For example, the $T_{\rm g}$ of the PEG-rich copolymer P_{25} was very low (-45 °C), whereas the $T_{\rm g}$ of the more rigid P_{100} , devoid of any PEG content, was much higher (+81 °C). The copolymer P₇₅ shows a pronounced and broad glass transition

centered around $-4\,^{\circ}\mathrm{C}$, which suggests that a majority of the material is a single amorphous phase, in addition to a faint transition at $-43\,^{\circ}\mathrm{C}$ that suggests the presence of a PEG-rich minority phase. The copolymers P_{25} and P_{50} are semicrystalline with melting temperatures of 32 and 34 $^{\circ}\mathrm{C}$, respectively, which is attributed to their higher content of PEG chains, which can form chain-folded crystallites. The polymerized curcumin units are unlikely to participate in crystallization because of the heterogeneity of the statistical copolymers. Although P_{100} might be possible to crystallize under some conditions, we did not observe a T_{m} transition by DSC under the conditions examined here (heat/cool/reheat with a ramp rate of 10 $^{\circ}\mathrm{C/min}$).

Film Surface Wettability, Swelling, and Mechanical **Properties.** Poly(curcumin-co-PEG) films were prepared by drop casting from chloroform solution (8% w/w) onto silicon substrates precleaned with atmospheric plasma. The films of the four copolymers exhibited distinct surface wetting behaviors as a result of their differences in copolymer composition. As expected, the hydrophobicity of the films increased with higher molar ratio of curcumin: P₁₀₀ was the most hydrophobic with a static water contact angle of 83.8 \pm 0.3° , whereas P_{75} films were slightly more hydrophilic, with a contact angle of $74.0 \pm 0.3^{\circ}$ (Figure 2A). It was not possible to obtain reliable equilibrium contact angle data for P25 and P50 films since these polymers are at least partially water-soluble and, thus, readily absorb the droplet of water. The water dissolution and swelling behavior of the films were then investigated by comparing the films' thicknesses in their dry state versus wet state. The very hydrophilic P_{25} , which has the highest PEG content, completely dissolves upon incubation in phosphate-buffered saline (PBS), as evidenced by the sudden decrease in film thickness from \sim 55 μ m to near-zero measurable thickness in the profilometer (Figure 2B). The film thickness for P₅₀ was significantly reduced in PBS because of its partial solubility in aqueous media. We propose that the partial solubility of P₅₀ is ascribed to the compositional dispersity in the random copolymer chains; a subpopulation of the sample that is more PEG-rich would exhibit better solubility than subpopulations that have PEG content less than the average of ~50% (Figure S2). Films of the more hydrophobic P₇₅ and P₁₀₀ showed no significant difference in thickness in their dry state versus wet state, which in combination with their relatively high contact angles, implies that no swelling or dissolution occurs in PBS.

Mechanical properties of poly(curcumin-co-PEG) thin films were studied by rheology (Figure 2C,D). At room temperature, P_{25} films have the highest storage modulus G' (7.3 MPa), which is consistent with the semicrystalline structure evidenced by DSC. P_{75} and P_{50} films were softer than P_{25} with G' values of 3.5 and 0.36 MPa, respectively. At 37 °C, the G'value for P25 quickly decreased and was lower than the loss modulus G'', thereby indicating the transition to a more liquidlike state at physiological temperature. A temperature sweep of P₂₅ from 25 to 42 °C shows the phase transition occurs at 31 °C under low strain, which is close to the melting point of 34 °C found by DSC (Figure S3). P₅₀ and P₇₅ films both became slightly softer at elevated temperature but remained predominately solidlike $(G' \gg G'')$ up to 42 °C. We were unable to obtain reliable rheological data of P_{100} because of the glassy brittleness of the film at room temperature, which is consistent with a $T_{\rm g}$ of 81 $^{\circ}{\rm C}$ via DSC.

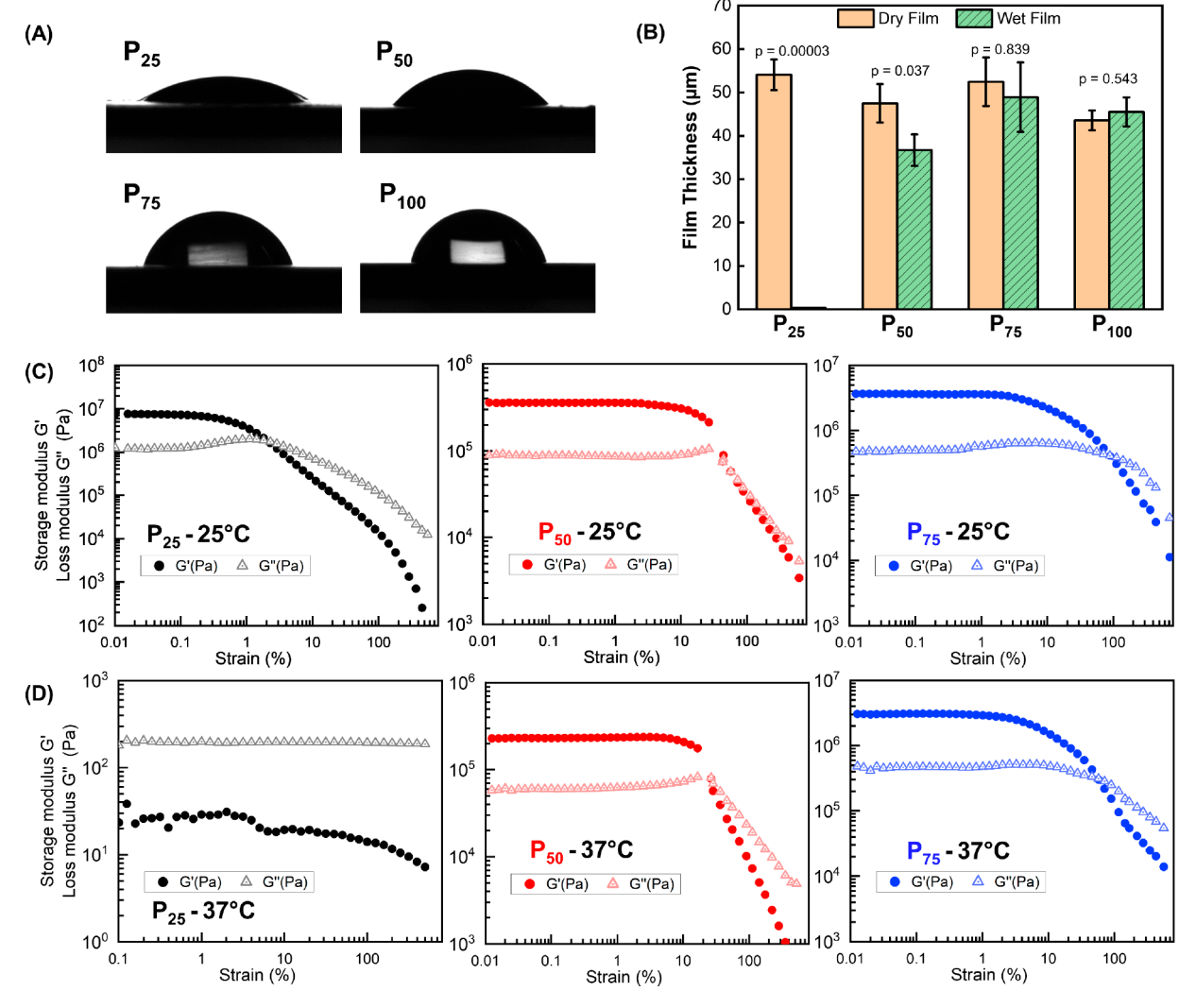


Figure 2. (A) Polymer film characterization by static water contact angle. Images were taken after 10 s of equilibration of a 3 μ L droplet. (B) Film thickness measured by profilometry. (C) Storage modulus (G') and loss modulus (G'') as a function of strain for P_{25} , P_{50} , and P_{75} , obtained at 25 °C (C) and 37 °C (D) at a constant frequency of 1 Hz.

Self-Assembly of P₅₀. The phenol groups in curcumin and the hydroxyl groups in PEG have different reactivities in the polycondensation reaction with sebacoyl chloride. This would presumably cause the two monomers to be consumed at different rates in a copolymerization reaction, thereby resulting in a compositional drift or blocky sequence. The more reactive monomer would preferentially be consumed in the earlier stage of polymerization, thereby leading to copolymers with very nonuniform sequence distributions. Although phenols are generally considered weaker nucleophiles than alcohols because of delocalization of the oxygen lone pair over the aromatic ring, we found curcumin to react much faster than PEG in condensation with sebacoyl chloride. This is supported by the observation that synthesis of P_{100} reached a molecular weight of 20 kDa within an hour, while P_{25} required 48 h to achieve a similar molecular weight. The sluggish reactivity of the hydroxyl end groups on PEG-1k could be attributed to the restricted availability of the end groups, which may be partially shielded within the entangled PEG chain in solution. It has been reported that block copolymers containing curcumin and PEG may undergo spontaneous organization of chain segments in selective solvents. 44,46 Although the poly(curcumin-co-PEG) copolymers we synthesized in this study are not strictly block copolymers, they may have the potential to form supramolecular assemblies under certain conditions. Indeed, this expectation was borne out in certain conditions.

SEM images of the four copolymer films drop-casted from chloroform showed that P_{100} was a smooth film, and P_{75} was textured on the micro/nano scale, whereas P₅₀ and P₂₅ contained micron-scale spherical inclusions within the thin film (Figure S4). The results suggest that self-assembly took place in chloroform solution, presumably driven by π stacking of curcumin and/or the solvophobic interaction between curcumin-rich segments and chloroform. In order to isolate the self-assembled objects for further analysis, we washed the copolymer films with deionized water, which removed some water-soluble components. The P25 film was fully dissolved; the P₁₀₀ and P₇₅ films were unchanged. Most interestingly, however, was that P₅₀ showed intermediate characteristics (Figure 3A,B): after the partial water-soluble fraction was washed out from the film, the remaining portion was spherical self-assembled objects with an average size of \sim 5 μ m. These spherical particles remained stable upon resuspension in water with sonication and could be injected through a 22G needle (Figure 3B). The particles persisted even after incubation in PBS at 37 °C for 6 months, which demonstrates excellent long-

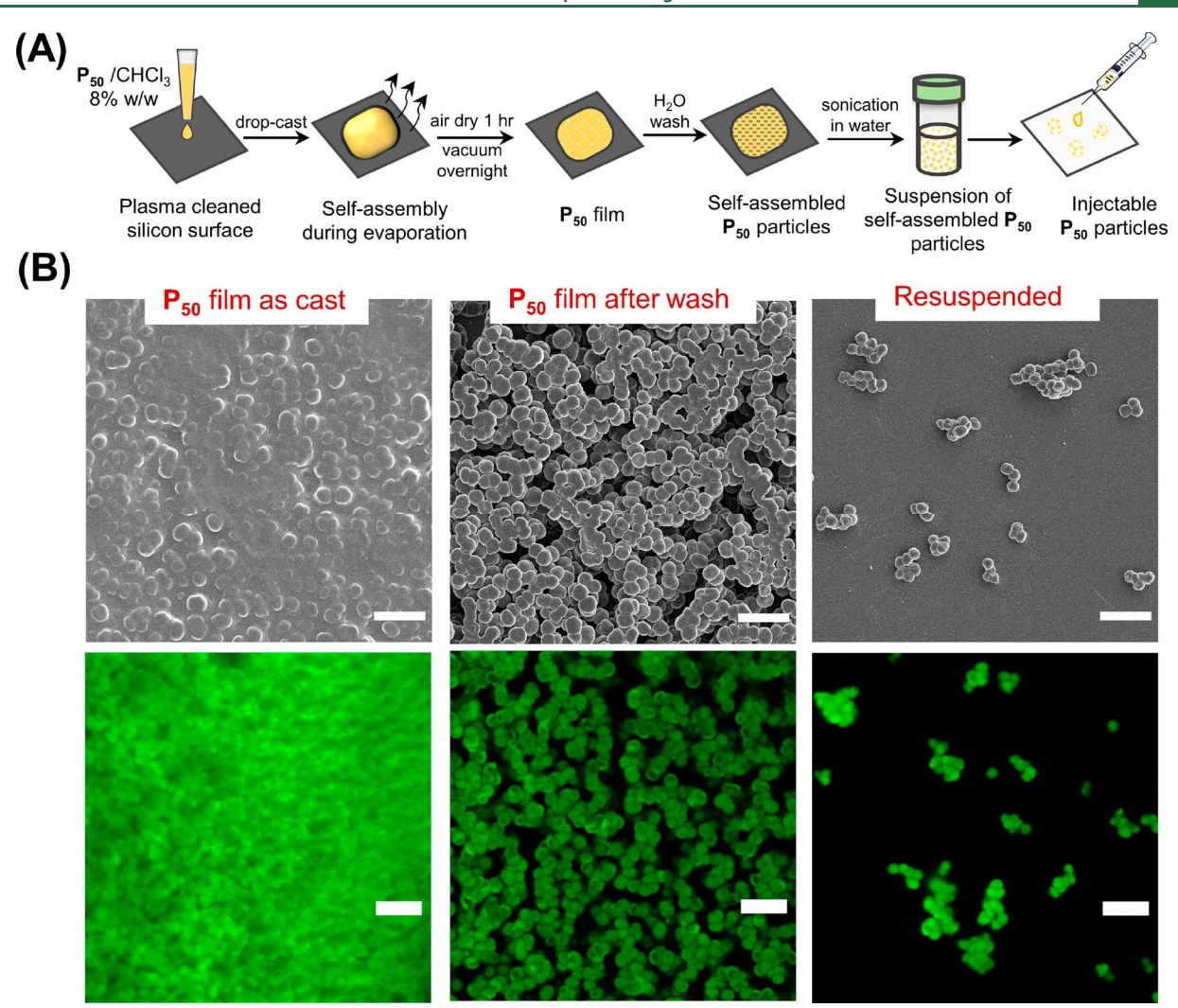


Figure 3. Self-assembly of P_{50} in evaporating chloroform solution generates spherical particles. (A) Schematic illustration of the drop-casting procedure. Drop-casted films were washed with water to remove water-soluble fractions. Remaining self-assembled particles were suspended in water by sonication and injected on glass coverslips through a 22G needle. (B) SEM and confocal images of as-cast P_{50} film, after wash, and after sonication and injection. All scale bars represent 20 μ m.

term stability. These materials are promising as both coatings and local injectable polyprodrug depots that offer controlled release of curcumin. P₅₀ self-assembled into different morphologies under different drop-casting conditions (Figure 4). At a low concentration of 3% w/w in chloroform, selfassembly favored apparently vesicular objects of $10-15 \mu m$ (Figure 4B). When cast from 8% w/w solution, smaller globular structures were obtained. When the concentration was increased further (15% w/w), only smooth films were observed without any spherical substructures (Figure S4). This capability of tuning the morphologies of self-assembled structures with casting conditions renders the polymerized curcumin materials excellent candidates as carriers for other cargo, in addition to their inherent antioxidant ability. Specifically, for P₅₀ vesicles, hydrophobic and hydrophilic drugs could be loaded simultaneously in the shell and core of the vesicle to perhaps enable codelivery of drugs from a carrier that is inherently antioxidant in nature. Although beyond the scope of this work, we intend to pursue these and related ideas in the future.

Drug Release Kinetics. Because of the presence of ester groups, copolymers of poly(curcumin-co-PEG) may undergo

hydrolytic degradation to release curcumin, oligomeric fragments of PEGylated curcumin, and/or curcumin oxidation byproducts. The kinetics of curcumin release from the copolymers were measured by incubating films of the four copolymers in PBS at 37 °C. At predetermined time points, the supernatant buffer was collected for analysis, and the amount of curcumin in the supernatant was calculated on the basis of the absorbance relative to a calibration curve. Native curcumin is highly unstable in PBS; it undergoes rapid auto-oxidation in the presence of water and dissolved oxygen, which produces a variety of byproducts on the time scale of minutes. 53-56 The composition of curcumin auto-oxidation products is related to the time of incubation and has been well studied by Schneider and co-workers. $^{57-61}$ Native, unmodified curcumin in aqueous solution has the maximum absorption at 423 nm, which decays significantly after just 10 min in PBS at 37 °C (Figure 5A). Following auto-oxidation, new absorption peaks appear at 227, 264, and 366 nm. These correspond to some of the known curcumin byproducts: biocyclopentadione, spiroepoxide, and vinylether, respectively.⁵⁹ In this context, curcumin that is released via hydrolytic degradation of the copolymers is subject to auto-oxidation and, thus, the supernatant will contain a

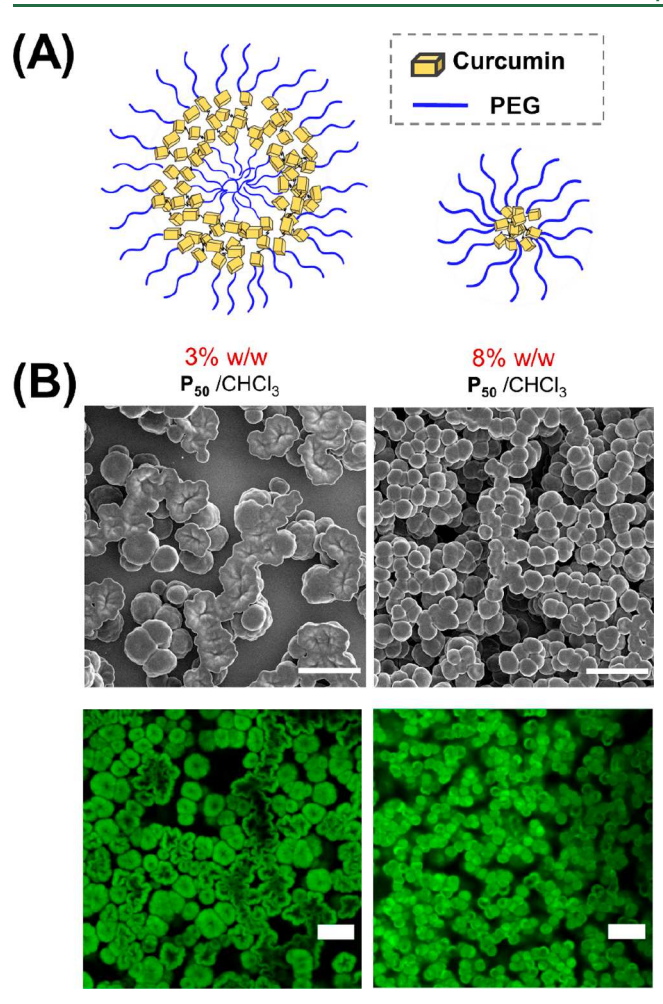


Figure 4. (A) Schematic illustration of the P_{50} self-assembly into putatively vesicular and/or globular structures. (B) SEM and confocal images of the self-assembled objects after drop-casting from 3% and 8% solution followed by H_2O wash. All scale bars represent 20 μ m.

mixture of curcumin's auto-oxidation byproducts. We selected the spiroepoxide product, which absorbs at 264 nm, as the reference peak for calibration because it is well resolved. A calibration curve was generated on the basis of the concentration of curcumin and intensity of absorbance at 264 nm after the curcumin solutions were incubated in PBS for 24 h to estimate the amount of curcumin released from the poly(curcumin-co-PEG) films. It is worth noting that the copolymer hydrolysis is a dynamic process, and the composition of the supernatant varies over time. We selected the calibration curve standards to be curcumin solutions in PBS after 24 h of degradation, but this method might underestimate the amount of curcumin released from the copolymers because degradation products other than 24 h were not included in the calculation.

We monitored the concentration of soluble spiroepoxide product from each of the films over 8 weeks (Figure 5B). The hydrophilic \mathbf{P}_{25} film was completely dissolved in PBS within 2 days. On the basis of the total amount of copolymer in the film and the molar ratio of curcumin within the copolymer, we calculated that 0.38 mg of curcumin equivalent is present initially. \mathbf{P}_{25} undergoes essentially complete burst release of soluble curcumin within a few days. On the opposite extreme, the more hydrophobic \mathbf{P}_{100} (lacking any PEG content) was found to release the curcumin spiroepoxide auto-oxidation

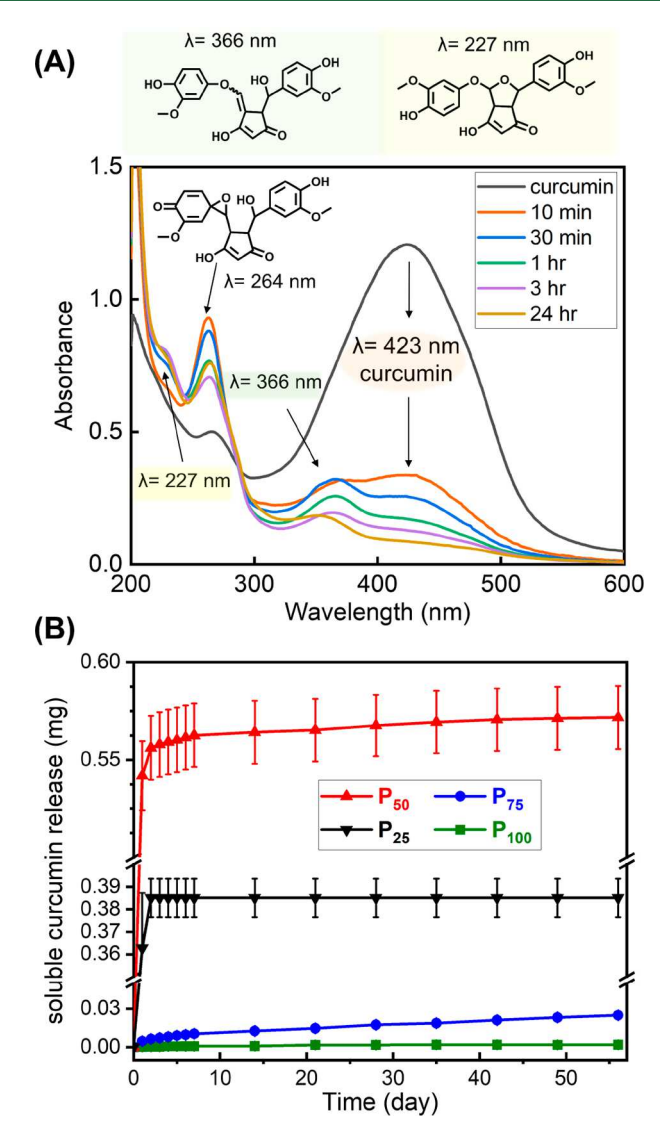


Figure 5. (A) Degradation of a 50 μ M curcumin solution in PBS over 24 h. (B) Soluble curcumin release from poly(curcumin-co-PEG) films. For P_{50} (>3 days), P_{75} , and P_{100} , calculation was based on the soluble spiroepoxide product released from the corresponding polymer films into PBS buffer. For water-soluble films P_{25} and P_{50} (<3 days), the amount of polymer dissolved was first calculated according to calibration curves of corresponding polymer in PBS, then the amount of curcumin was calculated on the basis of polymer composition. Plot of percentage release versus time can be found in Figure S5.

product at an almost imperceptibly slow pace, whereas P_{75} very gradually released 0.02 mg of curcumin over 8 weeks, which is only 1.6% of the total curcumin present in the film (Figure S5). Interestingly, the film of P_{50} , which is partially water-soluble and somewhat hydrophilic, showed the desired dual-stage release with an initial burst for the first few days followed by a gradual increase over the full 8-week duration. The initial dissolution of the water-soluble fraction of P_{50} gave a burst release of soluble curcumin of \sim 0.55 mg, which corresponds to approximately 66% of the total curcumin initially present in the film. The remaining intact copolymer film then underwent slow degradation and released trace amounts of curcumin byproduct in a sustained manner over 8 weeks. The total percentage of curcumin release at 8 week was 68%. Overall, the results show that varying the copolymer composition can

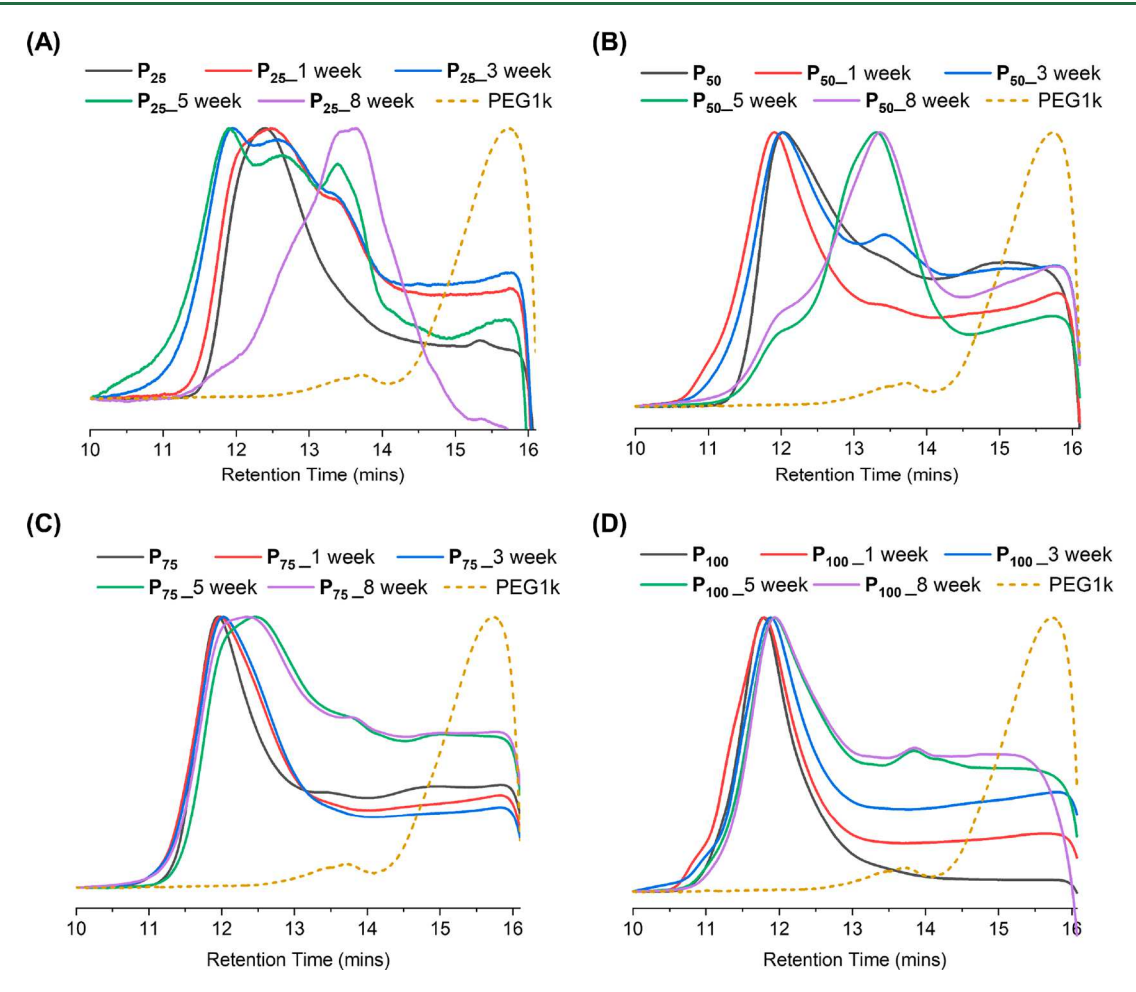


Figure 6. Degradation of poly(curcumin-co-PEG) observed by GPC. P_{25} samples for GPC were prepared by lyophilization of its aqueous solution after incubating for 1, 3, 5, and 8 weeks. P_{50} , P_{75} , and P_{100} samples were the remaining water-insoluble films after incubating in PBS for the corresponding duration and dissolving in THF for analysis. PEG1k trace was coplotted as a reference.

effectively tune the type and time scale of curcumin release from the thin film scaffold of the polymers.

Polymer Degradation. Changes in the molecular weight distributions (MWD) of the four copolymers following incubation in PBS at 37 °C for 1, 3, 5, and 8 weeks were characterized by GPC (Figure 6). Films of $P_{50}\!,\,P_{75}\!,$ and P_{100} were incubated in PBS at 37 °C, whereas the degradation of P_{25} was conducted in aqueous solutions because P_{25} is fully water-soluble. We found that 1 week and 3 week samples of all four polymers were not fully soluble in THF, which suggests that cross-linking and/or aggregation of the polymers occurs during incubation. The GPC traces of P25, P50, and P100, although only representative of the THF-soluble fraction of the remaining films, also showed a shift to lower retention time on the high MW side of the peak, which also indicates some initial cross-linking or aggregation. Perhaps cross-linking occurred via dimerization of curcumin following a radical mechanism in the presence of molecular oxygen, as Yamaguchi and co-workers have shown. 62 The four polymers' overall degradation rate is in agreement with their drug-release kinetics; P25 and P50 show a significant reduction in MW after 8 weeks, which indicates more hydrolytic degradation and greater curcumin release. Degradation of P_{25} and P_{50} was also shown by a reduction in absorbance at 400 nm (Figure S6). In contrast, P_{75} and P_{100} do not exhibit as pronounced a shift to higher MW, initially, but rather broaden more gradually on the low MW side of the

peak. By the end of the 8-week incubation, a substantial fraction of the P_{75} and P_{100} GPC chromatograms still have a peak around 12 min, which suggests that much of the polymer sample within the films remains completely unreacted at this time point. This also agrees with our observation of very slow, sustained release from P_{75} and P_{100} in Figure 5B.

Assessment of Hydrolysis Mechanism Using a Model **Compound.** The poly(curcumin-co-PEG) backbone consists of hydroxyl and phenolic esters that may undergo hydrolysis at different rates. Hydrolysis at the hydroxyl ester sites will release curcumin with the linker fragments, while hydrolysis from the phenolic esters would ultimately release whole curcumin. In order to compare the relative hydrolysis rate of the two esters, we synthesized a model compound 1 and studied its hydrolysis pathway by MALDI-TOF. The model compound was synthesized with one curcumin derivatized with 2 kDa monomethyl ether PEG on both ends via a two-carbon linker (Figure 7A). Unlike poly(curcumin-co-PEG) copolymers, which were highly polydisperse originating from the nature of step-growth polymerization, the model compound's polydispersity is narrow and arises only from the dispersity of the PEG 2k, itself. Hydrolysis of 1 will give three polymeric products 2, 3, and 4, which could be easily distinguished by MALDI-TOF-MS. We incubated a solution of 1 in PBS at 37 °C and collected an aliquot for MALDI analysis daily for 3 days. As shown in Figure 7B, the model compound was

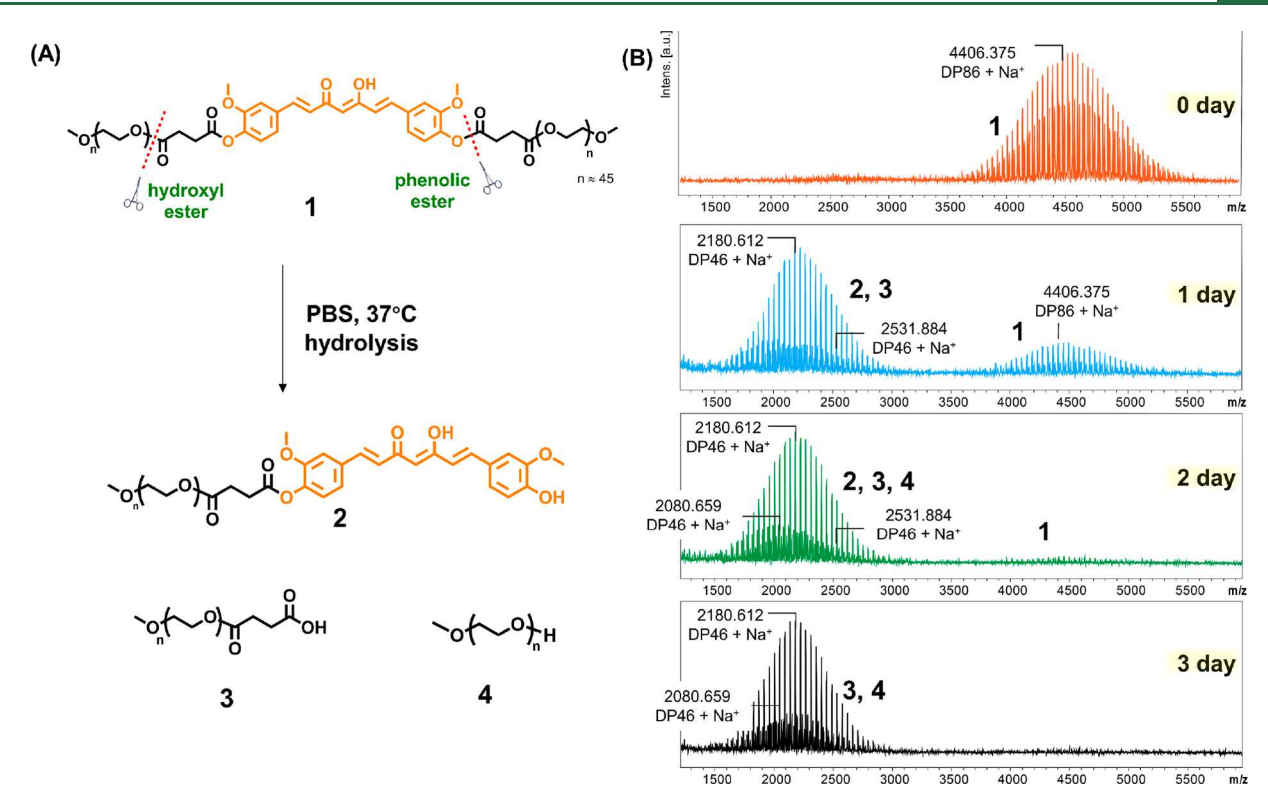


Figure 7. (A) Model compound 1 and predicted hydrolysis products. (B) MALDI data of 1 and hydrolysis products over 3 days at 37 °C. (MALDI mass lists and peak assignment can be found in Figure S7–10).

polydisperse with a peak molecular weight of 4406 Da, which closely matches the theoretical value of about 4 kDa. After 1 day of incubation, a large majority of 1 was broken down by hydrolysis, and hydrolysis exclusively took place at the phenolic esters, thereby giving degradation products of 2 and 3. After 2 days of incubation, very little of 1 was left in solution. Degradation product 4 was observed as a result of further hydrolysis of 2 and 3, but only at the later time point. After 3 days, all of 1 was degraded, and 2 was no longer observed in solution, either, as it underwent hydrolysis to give 3. Since 2 and 3 were first found during the hydrolysis of 1, and because 4 only appeared at a later time point, this suggests that the phenolic esters are more reactive than the hydroxyl esters and more prone to undergo hydrolysis first. This observation is consistent with the pK_a values of phenols (9.30 and 10.69 for curcumin)63,64 versus alcohols (15.9 for ethanol), which suggests phenols are better leaving groups in hydrolysis.

Radical Scavenging Activity. Curcumin is known to act as a free radical scavenger in solution. 2,62 A 2,2-diphenyl-1picrylhydrazyl free radical (DPPH) assay was performed with the P_{25} solution and P_{50} , P_{75} , P_{100} films to determine whether the copolymers in this study exhibit antioxidant activity. DPPH is a purple-colored persistent radical that absorbs light at 515 nm. In the presence of a radical scavenger, it abstracts a hydrogen atom, transforms into a nonradical form, and loses absorbance at 515 nm. The radical scavenging ability of a substance can be quantified on the basis of the reduction in absorbance.65-67 Quantitative DPPH assay was performed with P₂₅ because this polymer is fully soluble in PBS, which is in turn miscible with DPPH ethanol solution. When mixing P_{25} with DPPH, the absorption at 515 nm decreased in a concentration-dependent manner, thereby indicating that the P₂₅ polymer acts as a radical scavenger (Figure 8A). The

radical scavenging ability of P25 was also found to be longlasting (Figure 8B). The inhibition of DPPH• by P₂₅ dropped from 28% to 18% in the first week, then maintained around 18% in the following 7 weeks. The radical scavenging abilities of P₅₀, P₇₅, and P₁₀₀ were characterized with DPPH qualitatively because these materials were not soluble in the assay media but could quench some DPPH as insoluble solids in contact with DPPH solution (Figure 8C). Films of P_{50} showed strong antioxidant activity, which was visibly evident because the purple color of DPPH disappears in solution that is in contact with insoluble polymer films. This result could be attributed to the partial water solubility of P_{50} , which led to a burst release of soluble curcumin polymer, as described above. However, even after 3 months of incubation in PBS at 37 °C, the remaining P_{50} polymer film still showed strong antioxidant activity, which suggests that even the insoluble fraction remains active for prolonged times, even in heterogeneous contact with DPPH in solution. Although P_{100} contains the highest amount of antioxidant curcumin, it showed no antioxidant activity in this assay. The color change of DPPH solution with P_{100} films was hardly noticeable, presumably because P_{100} is too hydrophobic, and the heterogeneous reaction between the film and DPPH solution is likely very slow. P75 film had intermediate antioxidant activity, as compared with P50 and P_{100} , in which the purple color of DPPH solution was partially reduced, which is consistent with the drug release profile (Figure 5B). The copolymers P_{50} and P_{75} retained their antioxidant activity even after incubation in PBS at 37 °C for 3 and 6 months, respectively. This long-term antioxidant reactivity is useful for applications that require continued neutralization of reactive oxygen species (ROS) over extended time scales, such as in chronic wound healing or in the

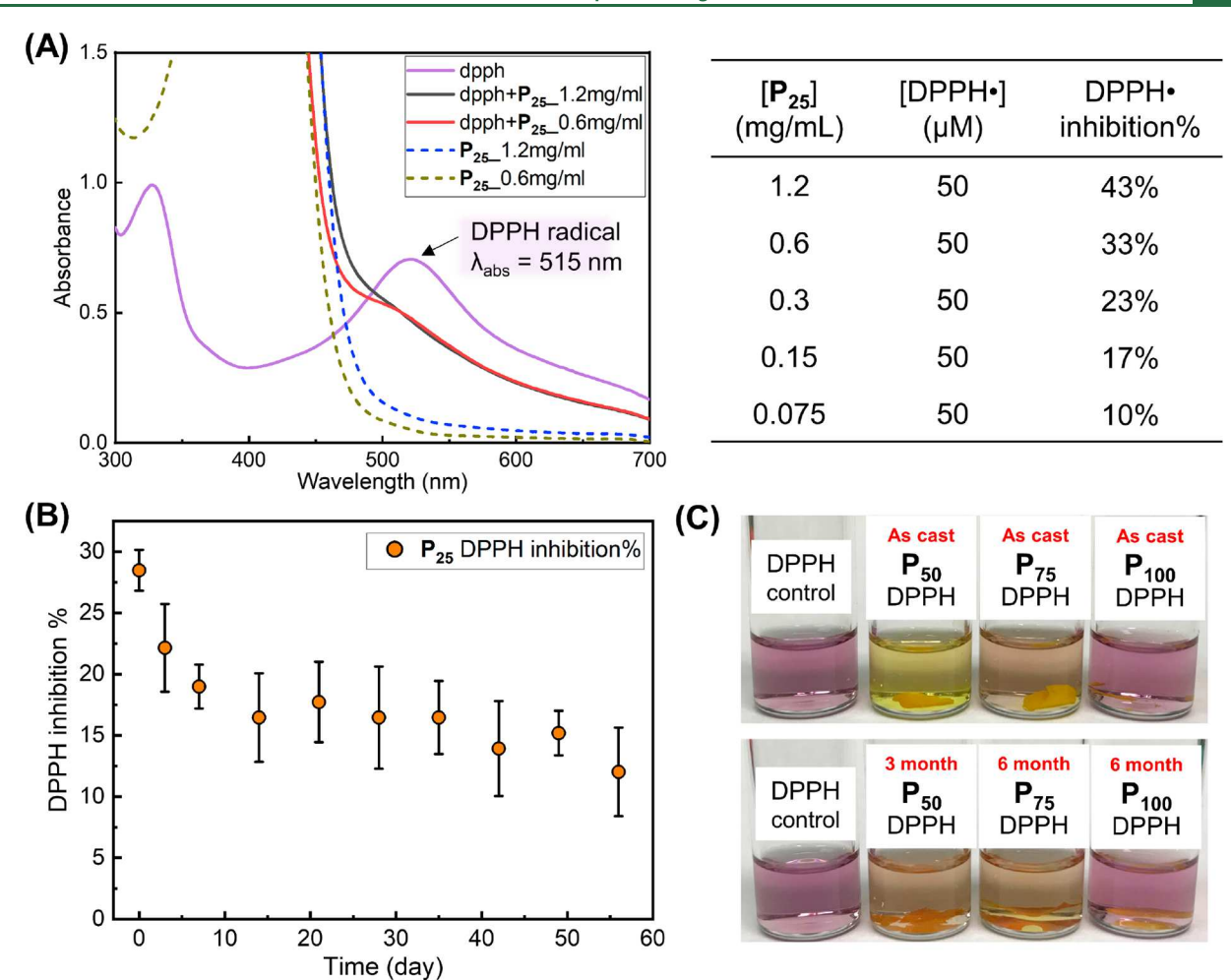


Figure 8. (A) P_{25} DPPH assay. P_{25} concentrations of 1.2–0.075 mg/mL with a constant [DPPH] = 50 μ M. (B) P_{25} DPPH inhibition % over 8 weeks. [P_{25}] = 0.5 mg/mL, [DPPH] = 50 μ M. (C) As-cast and degraded P_{50} , P_{75} , and P_{100} films (5 × 10 mm) combined with 1 mL of 50 μ M DPPH solution and reacted in dark for 30 min.

secondary injury cascade that occurs after injury to the central nervous system. $^{49,68-73}$

The structural element that contributes to curcumin's ability to scavenge free radicals has been a topic of controversial debate. 64,74-80 It was conventionally believed that the phenol groups contributed to the radical scavenging capability of curcumin by donating a hydrogen atom to radicals, thereby yielding resonance-stabilized phenolic radicals that are no longer able to undergo chain propagations. 74–76 Other studies argued that the methylene group at the center of curcumin was responsible for the antioxidant properties of curcumin, presumably following a sequential proton loss/electron transfer mechanism. 77,78,81 The latter process was thought to be dominant in polar solvents, such as alcohols and water. 64,79,80 In this study, the phenol groups on curcumin were polymerized in the copolymer, with the minor possible exception of curcumin on the chain ends. The aforementioned exception is likely insignificant, however, since curcumin is incorporated into the copolymer much faster than PEG, and therefore, at high conversion, one expects mainly PEG end groups to predominate. It is apparent that although the phenol groups on curcumin were mostly transformed into esters by polymerization, the copolymers still exhibited radical scavenging activity. This is reasonable since polar solvents such as water can promote the ionization of the enol (the most acidic

site in curcumin, $pK_a = 8.55$). ⁸⁰ A consequent electron transfer reaction would quench DPPH• free radicals. Another possible explanation for the radical scavenging capability of P_{25} is that the phenol groups on the polymer chain ends quench DPPH• by donating a hydrogen to DPPH•, although this is expected to play only a minor role, if any, for the reasons mentioned above.

Cytotoxicity and Hydrogen Peroxide Rescue Assay. The toxicity of the poly(curcumin-co-PEG) films, as well as their capability of quenching ROS to salvage neuronal viability, was assessed by incubating primary rat cortical neuronal cultures with solubilized P₂₅ films with and without a hydrogen peroxide insult (Figure 9A). The average weight of each polymer film was 5.04 ± 0.41 mg (Figure S11), which resulted in a final concentration of 10 mg/mL for each culture well since the P₂₅ polymer fully dissolved into the media after 24 h. There was no statistically significant change in cell viability with the presence of P₂₅ compared with the control (Figure 9B), which indicates that the polymer is nontoxic even at this very high concentration. The hydrogen peroxide insult significantly decreased neuronal viability to about 50% of the control value, while the P₂₅ film was able to rescue the decrease in viability to some extent as there was a significant increase in viability with the presence of the film compared with the hydrogen peroxide alone (Figure 9B). It is possible that the

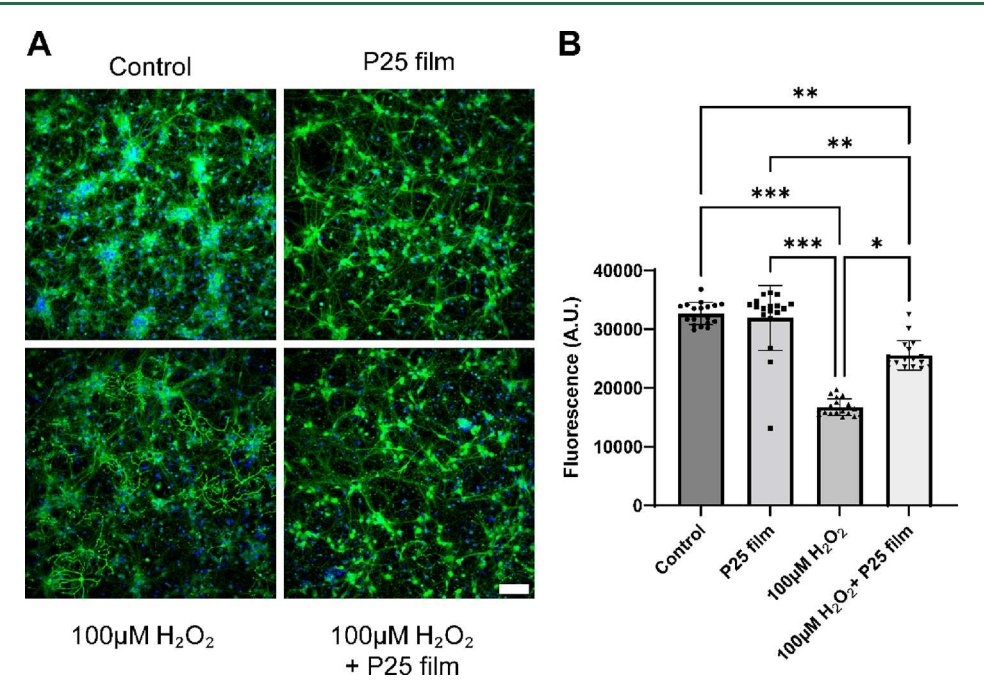


Figure 9. P_{25} films rescue cortical neuron viability from a hydrogen peroxide insult. (A) Representative images of primary rat cortical neuron cultures stained against neurofilament (green) and stained for all nuclei (blue). Cells were either treated with water (control), a P_{25} film, $100~\mu M$ H_2O_2 , or both $100~\mu M$ H_2O_2 and the P_{25} film added simultaneously (scale bar = $100~\mu m$). (B) Graph of mean arbitrary fluorescence units after 24 h of incubation with PrestoBlue cell viability reagent in each culture condition. Error bars indicate \pm standard deviation; each data point indicates fluorescence from one culture well. Statistical significance between groups was assessed using Kruskal–Wallis ANOVA and Dunn's post hoc test (*p < 0.05, **p < 0.01).

polymers with higher curcumin content may be able to fully rescue neuron viability but may be more cytotoxic at the same concentration because of lower PEG content. Future studies will more thoroughly investigate the details of the cytotoxicity of each of the polymers at various concentrations, as well as their neuronal rescue activities in vitro.

Curcumin is of interest as a neurotherapeutic because it has been shown to provide neuroprotection and improved functional outcomes following traumatic brain injury, spinal cord injury, Alzheimer's disease, and multiple sclerosis. 82-87 Many previous studies have also shown the benefits of utilizing various biomaterials, such as nanoparticles, liposomes, and biomimetic polymers, to increase the solubility of curcumin for more effective treatment of nervous system injury.^{85,88-93} However, these systems still rely on curcumin release and are limited by the amount of drug loading. To our knowledge, this study is the first to develop a poly(curcumin-co-PEG) that is fully water-soluble and capable of quenching free radicals and rescuing neuronal viability while still in its polymerized form. Furthermore, P₂₅ was able to continue quenching free radicals for 8 weeks. This longevity could be beneficial for treating chronic neural injury because inflammatory macrophages continue to produce ROS for months to years after traumatic brain injury and spinal cord injury.68-70 Neural probe implantation into the brain also elicits an oxidative stress and inflammatory response that compromises the implant functionality over time. 49 The more hydrophobic polymers developed in this study may allow for a stable coating material for brain implants that mitigates the foreign body response by attenuating ROS and inflammation. These polymers may also have a potential benefit for many other medical applications that involve ROS and inflammation, including bone 13,94 and

cardiac^{95,96} tissue engineering, wound dressings,^{71–73} and coatings for orthopedic implants.^{97,98}

CONCLUSION

In summary, we synthesized a series of poly(curcumin-co-PEG) with 25-100 mol % of curcumin loading by condensation polymerization and characterized the material properties, degradation behavior, and antioxidant activity. The hydrophilicities of the polymers increased with higher incorporation of the PEG segment, as expected. When incubated in buffer at 37 °C, films of these copolymers underwent hydrolytic degradation by ester hydrolysis and, thus, released curcumin gradually over long time periods, thereby enabling sustained antioxidant activity. We studied the relative reactivities of the phenolic ester and hydroxyl esters and found that the phenolic esters were prone to hydrolyze faster; this implies that curcumin itself, without the sebacoyl linker moiety, would be released preferentially. We found that curcumin release kinetics from the four polymers are related to their hydrophilicity: the more hydrophilic polymers released soluble curcumin primarily by dissolution and rapid hydrolysis, while the more hydrophobic polymers remained in their solid thin-film state and only released curcumin via gradual ester hydrolysis. The polymers exhibited long-term radical scavenging activities and were able to rescue cortical neuron viability from H₂O₂ insult. Poly(curcumin_{0.5}-co-PEG_{0.5}) self-assembled into vesicles and globular structures under adjustable conditions, thereby making it a potential candidate as a drug carrier. The unique properties of poly(curcumin-co-PEG), such as a tunable hydrophilicity based on curcumin loading, nonswelling surface properties, and a controllable release profile, suggest that these polymers may be used as coatings for

implants or as treatment modalities for chronic inflammation and tissue injury.

ASSOCIATED CONTENT

Supporting Information

The Supporting Information is available free of charge at https://pubs.acs.org/doi/10.1021/acs.biomac.2c01135.

Material and methods, including the synthesis of copolymers and model compound, fabrication of thin films and self-assembly, biological assays, and microscopy procedures (PDF)

AUTHOR INFORMATION

Corresponding Authors

Ryan J. Gilbert — Center for Biotechnology and Interdisciplinary Studies and Department of Biomedical Engineering, Rensselaer Polytechnic Institute, Troy, New York 12180, United States; Albany Stratton Veteran Affairs Medical Center, Albany, New York 12208, United States; orcid.org/0000-0002-3501-6753; Email: gilber2@rpi.edu

Edmund F. Palermo — Center for Biotechnology and Interdisciplinary Studies and Department of Materials Science and Engineering, Rensselaer Polytechnic Institute, Troy, New York 12180, United States; Occid.org/0000-0003-3656-787X; Email: palere@rpi.edu

Authors

Ruiwen Chen — Center for Biotechnology and Interdisciplinary Studies, Rensselaer Polytechnic Institute, Troy, New York 12180, United States

Jessica L. Funnell – Center for Biotechnology and Interdisciplinary Studies and Department of Biomedical Engineering, Rensselaer Polytechnic Institute, Troy, New York 12180, United States

Geraldine B. Quinones — Center for Biotechnology and Interdisciplinary Studies and Department of Biological Sciences, Rensselaer Polytechnic Institute, Troy, New York 12180, United States

Marvin Bentley — Center for Biotechnology and Interdisciplinary Studies and Department of Biological Sciences, Rensselaer Polytechnic Institute, Troy, New York 12180, United States

Jeffrey R. Capadona – Department of Biomedical Engineering, Case Western Reserve University, Cleveland, Ohio 44106, United States; Advanced Platform Technology Center, L. Stokes Cleveland VA Medical Center, Cleveland, Ohio 44106, United States

Complete contact information is available at: https://pubs.acs.org/10.1021/acs.biomac.2c01135

Notes

The authors declare no competing financial interest.

■ ACKNOWLEDGMENTS

The authors gratefully acknowledge the following funding sources: United States Department of Veteran's Affairs (I01RX003502-01A1) to R.J.G., E.F.P., and J.R.C.; the National Science Foundation (#2217513) to E.F.P. and R.J.G.; and a Research Career Scientist Award # GRANT12635707, to J.R.C., from the United States Department of Veterans Affairs Rehabilitation Research and Develop-

ment Service. This material is based upon work supported by the Department of Veterans Affairs, Veterans Health Administration, Office of Research and Development.

REFERENCES

- (1) Giordano, A.; Tommonaro, G. Curcumin and cancer. *Nutrients* **2019**, 11 (10), 2376.
- (2) Sharma, R. A.; Gescher, A. J.; Steward, W. P. Curcumin: The story so far. Eur. J. Cancer 2005, 41 (13), 1955-1968.
- (3) Lestari, M. L. A. D.; Indrayanto, G., Chapter three curcumin. In *Profiles of drug substances, excipients and related methodology*, Vol. 39; Brittain, H. G., Ed.; Academic Press, 2014; pp 113–204.
- (4) Hatcher, H.; Planalp, R.; Cho, J.; Torti, F. M.; Torti, S. V. Curcumin: From ancient medicine to current clinical trials. *Cell. Mol. Life Sci.* **2008**, *65* (11), 1631–1652.
- (5) Goel, A.; Kunnumakkara, A. B.; Aggarwal, B. B. Curcumin as "curecumin": From kitchen to clinic. *Biochem. Pharmacol.* **2008**, *75* (4), 787–809.
- (6) Hewlings, S. J.; Kalman, D. S. Curcumin: A review of its effects on human health. *Foods* **2017**, *6* (10), 92.
- (7) Caillaud, M.; Chantemargue, B.; Richard, L.; Vignaud, L.; Favreau, F.; Faye, P.-A.; Vignoles, P.; Sturtz, F.; Trouillas, P.; Vallat, J.-M.; et al. Local low dose curcumin treatment improves functional recovery and remyelination in a rat model of sciatic nerve crush through inhibition of oxidative stress. *Neuropharmacology* **2018**, *139*, 98–116.
- (8) Mythri, R. B.; Jagatha, B.; Pradhan, N.; Andersen, J.; Bharath, M. S. Mitochondrial complex i inhibition in parkinson's disease: How can curcumin protect mitochondria? *Antioxid. Redox Signal* **2007**, *9* (3), 399–408.
- (9) Hsu, C.-H.; Cheng, A.-L., Clinical studies with curcumin. In *The molecular targets and therapeutic uses of curcumin in health and disease*, Vol. 595; Springer, 2007; pp 471–480.
- (10) Anand, P.; Kunnumakkara, A. B.; Newman, R. A.; Aggarwal, B. B. Bioavailability of curcumin: Problems and promises. *Mol. Pharmaceutics* **2007**, *4* (6), 807–818.
- (11) Ng, Z. Y.; Wong, J.-Y.; Panneerselvam, J.; Madheswaran, T.; Kumar, P.; Pillay, V.; Hsu, A.; Hansbro, N.; Bebawy, M.; Wark, P.; Hansbro, P.; Dua, K.; Chellappan, D. K. Assessing the potential of liposomes loaded with curcumin as a therapeutic intervention in asthma. *Colloids Surf. B. Biointerfaces* **2018**, *172*, 51–59.
- (12) Huang, M.; Liang, C.; Tan, C.; Huang, S.; Ying, R.; Wang, Y.; Wang, Z.; Zhang, Y. Liposome co-encapsulation as a strategy for the delivery of curcumin and resveratrol. *Food Funct.* **2019**, *10* (10), 6447–6458.
- (13) Sarkar, N.; Bose, S. Liposome-encapsulated curcumin-loaded 3d printed scaffold for bone tissue engineering. ACS Appl. Mater. Interfaces 2019, 11 (19), 17184–17192.
- (14) Lübtow, M. M.; Nelke, L. C.; Seifert, J.; Kühnemundt, J.; Sahay, G.; Dandekar, G.; Nietzer, S. L.; Luxenhofer, R. Drug induced micellization into ultra-high capacity and stable curcumin nanoformulations: Physico-chemical characterization and evaluation in 2d and 3d in vitro models. *J. Controlled Release* **2019**, 303, 162–180.
- (15) Gupta, A.; Costa, A. P.; Xu, X.; Lee, S.-L.; Cruz, C. N.; Bao, Q.; Burgess, D. J. Formulation and characterization of curcumin loaded polymeric micelles produced via continuous processing. *Int. J. Pharm.* **2020**, 583, 119340.
- (16) Yallapu, M. M.; Jaggi, M.; Chauhan, S. C. Poly(β -cyclodextrin)/curcumin self-assembly: A novel approach to improve curcumin delivery and its therapeutic efficacy in prostate cancer cells. *Macromol. Biosci.* **2010**, *10* (10), 1141–1151.
- (17) Kasapoglu-Calik, M.; Ozdemir, M. Synthesis and controlled release of curcumin-β-cyclodextrin inclusion complex from nanocomposite poly(n-isopropylacrylamide/sodium alginate) hydrogels. J. Appl. Polym. Sci. 2019, 136 (21), 47554.
- (18) Chao, S.; Lv, X.; Ma, N.; Shen, Z.; Zhang, F.; Pei, Y.; Pei, Z. A supramolecular nanoprodrug based on a boronate ester linked

- curcumin complexing with water-soluble pillar[5]arene for synergistic chemotherapies. *Chem. Commun.* **2020**, *56* (62), 8861–8864.
- (19) Yallapu, M. M.; Jaggi, M.; Chauhan, S. C. Curcumin nanoformulations: A future nanomedicine for cancer. *Drug Discovery Today* **2012**, *17* (1–2), 71–80.
- (20) Shehzad, A.; Ul-Islam, M.; Wahid, F.; Lee, Y. S. Multifunctional polymeric nanocurcumin for cancer therapy. *J. Nanosci. Nanotechnol.* **2014**, *14* (1), 803–14.
- (21) Liu, Q.; Jing, Y.; Han, C.; Zhang, H.; Tian, Y. Encapsulation of curcumin in zein/ caseinate/sodium alginate nanoparticles with improved physicochemical and controlled release properties. *Food Hydrocoll.* **2019**, 93, 432–442.
- (22) Liu, Q.; Han, C.; Tian, Y.; Liu, T. Fabrication of curcumin-loaded zein nanoparticles stabilized by sodium caseinate/sodium alginate: Curcumin solubility, thermal properties, rheology, and stability. *Process Biochem.* **2020**, *94*, 30–38.
- (23) Tian, Y.; Jia, D.; Dirican, M.; Cui, M.; Fang, D.; Yan, C.; Xie, J.; Liu, Y.; Li, C.; Fu, J.; Liu, H.; Chen, G.; Zhang, X.; Tao, J. Highly soluble and stable, high release rate nanocellulose codrug delivery system of curcumin and aunps for dual chemo-photothermal therapy. *Biomacromolecules* **2022**, 23 (3), 960–971.
- (24) Elbialy, N. S.; Aboushoushah, S. F.; Sofi, B. F.; Noorwali, A. Multifunctional curcumin-loaded mesoporous silica nanoparticles for cancer chemoprevention and therapy. *Microporous Mesoporous Mater.* **2020**, *291*, 109540.
- (25) Luckanagul, J. A.; Ratnatilaka Na Bhuket, P.; Muangnoi, C.; Rojsitthisak, P.; Wang, Q.; Rojsitthisak, P. Self-assembled thermoresponsive nanogel from grafted hyaluronic acid as a biocompatible delivery platform for curcumin with enhanced drug loading and biological activities. *Polymers* **2021**, *13* (2), 194.
- (26) Kamaly, N.; Yameen, B.; Wu, J.; Farokhzad, O. C. Degradable controlled-release polymers and polymeric nanoparticles: Mechanisms of controlling drug release. *Chem. Rev.* **2016**, *116* (4), 2602–2663.
- (27) Pan, R.; Liu, G.; Li, Y.; Wei, Y.; Li, S.; Tao, L. Size-dependent endocytosis and a dynamic-release model of nanoparticles. *Nanoscale* **2018**, *10* (17), 8269–8274.
- (28) Ekladious, I.; Colson, Y. L.; Grinstaff, M. W. Polymer-drug conjugate therapeutics: Advances, insights and prospects. *Nat. Rev. Drug Discovery* **2019**, *18* (4), 273–294.
- (29) Zhang, G.; Li, X.; Liao, Q.; Liu, Y.; Xi, K.; Huang, W.; Jia, X. Water-dispersible peg-curcumin/amine-functionalized covalent organic framework nanocomposites as smart carriers for in vivo drug delivery. *Nat. Commun.* **2018**, 9 (1), 2785.
- (30) Tang, H.; Murphy, C. J.; Zhang, B.; Shen, Y.; Sui, M.; Kirk, E. A. V.; Feng, X.; Murdoch, W. J. Amphiphilic curcumin conjugate-forming nanoparticles as anticancer prodrug and drug carriers: In vitro and in vivo effects. *Nanomedicine* **2010**, *5* (6), 855–865.
- (31) Fan, Z.; Li, J.; Liu, J.; Jiao, H.; Liu, B. Anti-inflammation and joint lubrication dual effects of a novel hyaluronic acid/curcumin nanomicelle improve the efficacy of rheumatoid arthritis therapy. ACS Appl. Mater. Interfaces 2018, 10 (28), 23595–23604.
- (32) Li, J.; Shin, G. H.; Chen, X.; Park, H. J. Modified curcumin with hyaluronic acid: Combination of pro-drug and nano-micelle strategy to address the curcumin challenge. *Food Res. Int.* **2015**, *69*, 202–208.
- (33) Guo, C.; Hou, X.; Liu, Y.; Zhang, Y.; Xu, H.; Zhao, F.; Chen, D. Novel chinese angelica polysaccharide biomimetic nanomedicine to curcumin delivery for hepatocellular carcinoma treatment and immunomodulatory effect. *Phytomedicine* **2021**, *80*, 153356.
- (34) Hassani, A.; Mahmood, S.; Enezei, H. H.; Hussain, S. A.; Hamad, H. A.; Aldoghachi, A. F.; Hagar, A.; Doolaanea, A. A.; Ibrahim, W. N. Formulation, characterization and biological activity screening of sodium alginate-gum arabic nanoparticles loaded with curcumin. *Molecules* **2020**, 25 (9), 2244.
- (35) Sauraj; Kumar, V.; Kumar, B.; Priyadarshi, R.; Deeba, F.; Kulshreshtha, A.; Kumar, A.; Agrawal, G.; Gopinath, P.; Negi, Y. S. Redox responsive xylan-SS-curcumin prodrug nanoparticles for dual drug delivery in cancer therapy. *Mater. Sci. Eng., C* **2020**, *107*, 110356.
- (36) Pan, R.; Zeng, Y.; Liu, G.; Wei, Y.; Xu, Y.; Tao, L. Curcumin-polymer conjugates with dynamic boronic acid ester linkages for

- selective killing of cancer cells. *Polym. Chem.* **2020**, *11* (7), 1321–1326.
- (37) Pan, R.; Liu, G.; Zeng, Y.; He, X.; Ma, Z.; Wei, Y.; Chen, S.; Yang, L.; Tao, L. A multi-responsive self-healing hydrogel for controlled release of curcumin. *Polym. Chem.* **2021**, *12* (16), 2457–2463.
- (38) Averick, A.; Dolai, S.; Punia, A.; Punia, K.; Guariglia, S. R.; L'Amoreaux, W.; Hong, K.-l.; Raja, K. Green anchors: Chelating properties of atrp-click curcumin-polymer conjugates. *React. Funct. Polym.* **2016**, *102*, 47–52.
- (39) Vonnie, J. M.; Jing Ting, B.; Rovina, K.; Erna, K. H.; Felicia, W. X. L.; Nur 'Aqilah, N. M.; Abdul Wahab, R. Development of aloe veragreen banana saba-curcumin composite film for colorimetric detection of ferrum (ii). *Polymers* **2022**, *14* (12), 2353.
- (40) Seidi, F.; Jenjob, R.; Crespy, D. Designing smart polymer conjugates for controlled release of payloads. *Chem. Rev.* **2018**, *118* (7), 3965–4036.
- (41) Seidi, F.; Zhong, Y.; Xiao, H.; Jin, Y.; Crespy, D. Degradable polyprodrugs: Design and therapeutic efficiency. *Chem. Soc. Rev.* **2022**, *51* (15), 6652–6703.
- (42) Requejo-Aguilar, R.; Alastrue-Agudo, A.; Cases-Villar, M.; Lopez-Mocholi, E.; England, R.; Vicent, M. J.; Moreno-Manzano, V. Combined polymer-curcumin conjugate and ependymal progenitor/stem cell treatment enhances spinal cord injury functional recovery. *Biomaterials* **2017**, *113*, 18–30.
- (43) Tang, H.; Murphy, C. J.; Zhang, B.; Shen, Y.; Van Kirk, E. A.; Murdoch, W. J.; Radosz, M. Curcumin polymers as anticancer conjugates. *Biomaterials* **2010**, *31* (27), 7139–7149.
- (44) Qiao, Z.; Liu, H.-Y.; Zha, J.-C.; Mao, X.-X.; Yin, J. Completely degradable backbone-type hydrogen peroxide responsive curcumin copolymer: Synthesis and synergistic anticancer investigation. *Polym. Chem.* **2019**, *10* (31), 4305–4313.
- (45) Shpaisman, N.; Sheihet, L.; Bushman, J.; Winters, J.; Kohn, J. One-step synthesis of biodegradable curcumin-derived hydrogels as potential soft tissue fillers after breast cancer surgery. *Biomacromolecules* **2012**, *13* (8), 2279–2286.
- (46) Yu, F.; Tu, Y.; Luo, S.; Xiao, X.; Yao, W.; Jiang, M.; Jiang, X.; Yang, R.; Yuan, Y. Dual-drug backboned polyprodrug with a predefined drug combination for synergistic chemotherapy. *Nano Lett.* **2021**, *21* (5), 2216–2223.
- (47) Oprea, S.; Potolinca, V. O.; Oprea, V. Synthesis and characterization of novel polyurethane elastomers that include curcumin with various cross-linked structures. *J. Polym. Res.* **2020**, 27 (3), 60.
- (48) Matsumi, N.; Nakamura, N.; Aoi, K. Novel bio-based polyesters derived from curcumin as an inherent natural diol monomer. *Polym. J.* **2008**, *40* (5), 400–401.
- (49) Ereifej, E. S.; Rial, G. M.; Hermann, J. K.; Smith, C. S.; Meade, S. M.; Rayyan, J. M.; Chen, K.; Feng, H.; Capadona, J. R. Implantation of neural probes in the brain elicits oxidative stress. *Front. Bioeng. Biotechnol.* **2018**, *6*, 9.
- (50) Gaire, J.; Lee, H. C.; Hilborn, N.; Ward, R.; Regan, M.; Otto, K. J. The role of inflammation on the functionality of intracortical microelectrodes. *J. Neural Eng.* **2018**, *15* (6), 066027.
- (51) Salatino, J. W.; Ludwig, K. A.; Kozai, T. D.; Purcell, E. K. Glial responses to implanted electrodes in the brain. *Nat. Biomed. Eng.* **2017**, *1* (11), 862–877.
- (52) Ginés, J. M.; Arias, M. J.; Rabasco, A. M.; Novák, C.; Ruiz-Conde, A.; Sánchez-Soto, P. J. Thermal characterization of polyethylene glycols applied in the pharmaceutical technology using differential scanning calorimetry and hot stage microscopy. *J. Therm. Anal.* 1996, 46 (1), 291–304.
- (53) Wang, Y.-J.; Pan, M.-H.; Cheng, A.-L.; Lin, L.-I.; Ho, Y.-S.; Hsieh, C.-Y.; Lin, J.-K. Stability of curcumin in buffer solutions and characterization of its degradation products. *J. Pharm. Biomed. Anal.* **1997**, *15* (12), 1867–1876.
- (54) Tønnesen, H. H.; Karlsen, J. Studies on curcumin and curcuminoids. *Zeitschrift für Lebensmittel-Untersuchung und Forschung* 1985, 180 (5), 402–404.

- (55) Pfeiffer, E.; Höhle, S.; Solyom, A. M.; Metzler, M. Studies on the stability of turmeric constituents. *J. Food Eng.* **2003**, *56* (2), 257–259
- (56) Zhu, J.; Sanidad, K. Z.; Sukamtoh, E.; Zhang, G. Potential roles of chemical degradation in the biological activities of curcumin. *Food Funct.* **2017**, *8* (3), 907–914.
- (57) Griesser, M.; Pistis, V.; Suzuki, T.; Tejera, N.; Pratt, D. A.; Schneider, C. Autoxidative and cyclooxygenase-2 catalyzed transformation of the dietary chemopreventive agent curcumin*. *J. Biol. Chem.* **2011**, 286 (2), 1114–1124.
- (58) Gordon, O. N.; Schneider, C. Vanillin and ferulic acid: Not the major degradation products of curcumin. *Trends Mol. Med.* **2012**, *18* (7), 361–363.
- (59) Gordon, O. N.; Luis, P. B.; Sintim, H. O.; Schneider, C. Unraveling curcumin degradation: Autoxidation proceeds through spiroepoxide and vinylether intermediates en route to the main bicyclopentadione*. *J. Biol. Chem.* **2015**, 290 (8), 4817–4828.
- (60) Schneider, C.; Gordon, O. N.; Edwards, R. L.; Luis, P. B. Degradation of curcumin: From mechanism to biological implications. *J. Agric. Food. Chem.* **2015**, *63* (35), 7606–7614.
- (61) Joseph, A. I.; Luis, P. B.; Schneider, C. A curcumin degradation product, 7-norcyclopentadione, formed by aryl migration and loss of a carbon from the heptadienedione chain. *J. Nat. Prod.* **2018**, *81* (12), 2756–2762.
- (62) Masuda, T.; Hidaka, K.; Shinohara, A.; Maekawa, T.; Takeda, Y.; Yamaguchi, H. Chemical studies on antioxidant mechanism of curcuminoid: Analysis of radical reaction products from curcumin. *J. Agric. Food. Chem.* **1999**, *47* (1), 71–77.
- (63) Borsari, M.; Ferrari, E.; Grandi, R.; Saladini, M. Curcuminoids as potential new iron-chelating agents: Spectroscopic, polarographic and potentiometric study on their fe(iii) complexing ability. *Inorg. Chim. Acta* **2002**, 328 (1), 61–68.
- (64) Litwinienko, G.; Ingold, K. U. Abnormal solvent effects on hydrogen atom abstraction. 2. Resolution of the curcumin antioxidant controversy. The role of sequential proton loss electron transfer. *J. Org. Chem.* **2004**, *69* (18), 5888–5896.
- (65) Molyneux, P. The use of the stable free radical diphenylpicrylhydrazyl (dpph) for estimating antioxidant activity. *Songklanakarin J. sci. technol* **2004**, *26* (2), 211–219.
- (66) Sharma, O. P.; Bhat, T. K. Dpph antioxidant assay revisited. Food Chem. 2009, 113 (4), 1202-1205.
- (67) Pyrzynska, K.; Pękal, A. Application of free radical diphenylpicrylhydrazyl (dpph) to estimate the antioxidant capacity of food samples. *Anal. Methods* **2013**, *5* (17), 4288–4295.
- (68) Lewen, A.; Matz, P.; Chan, P. H. Free radical pathways in cns injury. J. Neurotrauma 2000, 17 (10), 871-890.
- (69) Gensel, J. C.; Zhang, B. Macrophage activation and its role in repair and pathology after spinal cord injury. *Brain Res.* **2015**, *1619*,
- (70) O'Connell, K. M.; Littleton-Kearney, M. T. The role of free radicals in traumatic brain injury. *Biol. Res. Nurs.* **2013**, *15* (3), 253–263
- (71) Ternullo, S.; Schulte Werning, L. V.; Holsæter, A. M.; Škalko-Basnet, N. Curcumin-in-deformable liposomes-in-chitosan-hydrogel as a novel wound dressing. *Pharmaceutics* **2020**, *12* (1), 8.
- (72) Sadeghianmaryan, A.; Yazdanpanah, Z.; Soltani, Y. A.; Sardroud, H. A.; Nasirtabrizi, M. H.; Chen, X. Curcumin-loaded electrospun polycaprolactone/montmorillonite nanocomposite: Wound dressing application with anti-bacterial and low cell toxicity properties. *J. Biomater. Sci. Polym. Ed.* **2020**, 31 (2), 169–187.
- (73) Chen, K.; Pan, H.; Ji, D.; Li, Y.; Duan, H.; Pan, W. Curcuminloaded sandwich-like nanofibrous membrane prepared by electrospinning technology as wound dressing for accelerate wound healing. *Mater. Sci. Eng.*, C 2021, 127, 112245.
- (74) Barclay, L. R. C.; Vinqvist, M. R.; Mukai, K.; Goto, H.; Hashimoto, Y.; Tokunaga, A.; Uno, H. On the antioxidant mechanism of curcumin: Classical methods are needed to determine antioxidant mechanism and activity. *Org. Lett.* **2000**, *2* (18), 2841–2843.

- (75) Feng, J.-Y.; Liu, Z.-Q. Phenolic and enolic hydroxyl groups in curcumin: Which plays the major role in scavenging radicals? *J. Agric. Food. Chem.* **2009**, *57* (22), 11041–11046.
- (76) Priyadarsini, K. I.; Maity, D. K.; Naik, G. H.; Kumar, M. S.; Unnikrishnan, M. K.; Satav, J. G.; Mohan, H. Role of phenolic o-h and methylene hydrogen on the free radical reactions and antioxidant activity of curcumin. *Free Radical Biol. Med.* **2003**, *35* (5), 475–484.
- (77) Jovanovic, S. V.; Steenken, S.; Boone, C. W.; Simic, M. G. Hatom transfer is a preferred antioxidant mechanism of curcumin. *J. Am. Chem. Soc.* **1999**, *121* (41), 9677–9681.
- (78) Jovanovic, S. V.; Boone, C. W.; Steenken, S.; Trinoga, M.; Kaskey, R. B. How curcumin works preferentially with water soluble antioxidants. *J. Am. Chem. Soc.* **2001**, *123* (13), 3064–3068.
- (79) Litwinienko, G.; Ingold, K. U. Abnormal solvent effects on hydrogen atom abstractions. 1. The reactions of phenols with 2,2-diphenyl-1-picrylhydrazyl (dpph●) in alcohols. *J. Org. Chem.* **2003**, 68 (9), 3433−3438.
- (80) Foti, M. C. Antioxidant properties of phenols. *J. Pharm. Pharmacol.* **2010**, *59* (12), 1673–1685.
- (81) Foti, M. C.; Daquino, C.; Geraci, C. Electron-transfer reaction of cinnamic acids and their methyl esters with the dpph• radical in alcoholic solutions. *J. Org. Chem.* **2004**, *69* (7), 2309–2314.
- (82) Di Meo, F.; Margarucci, S.; Galderisi, U.; Crispi, S.; Peluso, G. Curcumin, gut microbiota, and neuroprotection. *Nutrients* **2019**, *11* (10), 2426.
- (83) Dong, W.; Yang, B.; Wang, L.; Li, B.; Guo, X.; Zhang, M.; Jiang, Z.; Fu, J.; Pi, J.; Guan, D.; et al. Curcumin plays neuroprotective roles against traumatic brain injury partly via nrf2 signaling. *Toxicol. Appl. Pharmacol.* **2018**, 346, 28–36.
- (84) Farkhondeh, T.; Samarghandian, S.; Roshanravan, B.; Peivasteh-Roudsari, L. Impact of curcumin on traumatic brain injury and involved molecular signaling pathways. *Recent Pat. Food Nutr. Agric.* **2020**, *11* (2), 137–144.
- (85) Mohajeri, M.; Sadeghizadeh, M.; Najafi, F.; Javan, M. Polymerized nano-curcumin attenuates neurological symptoms in eae model of multiple sclerosis through down regulation of inflammatory and oxidative processes and enhancing neuroprotection and myelin repair. *Neuropharmacology* **2015**, *99*, 156–167.
- (86) Reddy, P. H.; Manczak, M.; Yin, X.; Grady, M. C.; Mitchell, A.; Tonk, S.; Kuruva, C. S.; Bhatti, J. S.; Kandimalla, R.; Vijayan, M.; et al. Protective effects of indian spice curcumin against amyloid- β in alzheimer's disease. *J. Alzheimer's Dis.* **2018**, *61* (3), 843–866.
- (87) Yuan, J.; Zou, M.; Xiang, X.; Zhu, H.; Chu, W.; Liu, W.; Chen, F.; Lin, J. Curcumin improves neural function after spinal cord injury by the joint inhibition of the intracellular and extracellular components of glial scar. *J. Surg. Res.* **2015**, *195* (1), 235–245.
- (88) Yavarpour-Bali, H.; Ghasemi-Kasman, M.; Pirzadeh, M. Curcumin-loaded nanoparticles: A novel therapeutic strategy in treatment of central nervous system disorders. *Int. J. Nanomedicine* **2019**, *14*, 4449.
- (89) Schmitt, C.; Lechanteur, A.; Cossais, F.; Bellefroid, C.; Arnold, P.; Lucius, R.; Held-Feindt, J.; Piel, G.; Hattermann, K. Liposomal encapsulated curcumin effectively attenuates neuroinflammatory and reactive astrogliosis reactions in glia cells and organotypic brain slices. *Int. J. Nanomedicine* **2020**, *15*, 3649.
- (90) Li, L.; Zhang, X.; Pi, C.; Yang, H.; Zheng, X.; Zhao, L.; Wei, Y. Review of curcumin physicochemical targeting delivery system. *Int. J. Nanomedicine* **2020**, *15*, 9799.
- (91) Karthikeyan, A.; Senthil, N.; Min, T. Nanocurcumin: A promising candidate for therapeutic applications. *Front. Pharmacol.* **2020**, *11*, 487.
- (92) Sinclair, S. M.; Bhattacharyya, J.; McDaniel, J. R.; Gooden, D. M.; Gopalaswamy, R.; Chilkoti, A.; Setton, L. A. A genetically engineered thermally responsive sustained release curcumin depot to treat neuroinflammation. *J. Controlled Release* **2013**, *171* (1), 38–47.
- (93) He, R.; Jiang, Y.; Shi, Y.; Liang, J.; Zhao, L. Curcumin-laden exosomes target ischemic brain tissue and alleviate cerebral ischemia-reperfusion injury by inhibiting ros-mediated mitochondrial apoptosis. *Mater. Sci. Eng., C* **2020**, *117*, 111314.

- (94) Peddada, K. V.; Peddada, K. V.; Shukla, S. K.; Mishra, A.; Verma, V. Role of curcumin in common musculoskeletal disorders: A review of current laboratory, translational, and clinical data. *Orthop. Surg.* **2015**, *7* (3), 222–231.
- (95) Helli, B.; Gerami, H.; Kavianpour, M.; Heybar, H.; Hosseini, S. K.; Haghighian, H. K. Curcumin nanomicelle improves lipid profile, stress oxidative factors and inflammatory markers in patients undergoing coronary elective angioplasty; a randomized clinical trial. *Endocr. Metab. Immune. Disord. Drug Targets.* **2021**, *21* (11), 2090–2098.
- (96) Kargozar, S.; Baino, F.; Hoseini, S. J.; Verdi, J.; Asadpour, S.; Mozafari, M. Curcumin: Footprints on cardiac tissue engineering. *Expert Opin. Biol. Ther.* **2019**, *19* (11), 1199–1205.
- (97) Virk, R. S.; Rehman, M. A. U.; Munawar, M. A.; Schubert, D. W.; Goldmann, W. H.; Dusza, J.; Boccaccini, A. R. Curcumin-containing orthopedic implant coatings deposited on poly-ether-ether-ketone/bioactive glass/hexagonal boron nitride layers by electrophoretic deposition. *Coatings* **2019**, *9* (9), 572.
- (98) Sarkar, N.; Bose, S. Controlled delivery of curcumin and vitamin k2 from hydroxyapatite-coated titanium implant for enhanced in vitro chemoprevention, osteogenesis, and in vivo osseointegration. ACS Appl. Mater. Interfaces 2020, 12 (12), 13644–13656.

☐ Recommended by ACS

Two-Stage Supramolecular Self-Assembly-Directed Collagen-Peptide-Decorated Liposomal Complexes of Curcumin Microspheres with Enhanced Solubility and Bi...

Maria Jose Louis, Krishnakumar Illathu Madhavamenon, et al.

JULY 11, 2023 ACS OMEGA

READ 🗹

Curcumin-Loaded Macrophage-Derived Exosomes Effectively Improve Wound Healing

Daoyong Li, Xifan Mei, et al.

AUGUST 01, 2023

MOLECULAR PHARMACEUTICS

READ 🗹

Lactoferrin-Based Ternary Composite Nanoparticles with Enhanced Dispersibility and Stability for Curcumin Delivery

Xueqi Li, Fuguo Liu, et al.

MARCH 09, 2023

ACS APPLIED MATERIALS & INTERFACES

RFAD **「**✓

Carboxymethylpachymaran-Coated Zein Nanoparticles for Oral Delivery of Curcumin: Formation, Characterization, Physicochemical Stability, and Controlled Release Properties

Lan Wang, Jie Shi, et al.

JANUARY 04, 2023

ACS FOOD SCIENCE & TECHNOLOGY

READ 🗹

Get More Suggestions >